ELSEVIER

Cardiovascular Research 70 (2006) 509 – 520

Cardiovascular Research

www.elsevier.com/locate/cardiores

Incorporated sarcolemmal fish oil fatty acids shorten pig ventricular action potentials

Arie O. Verkerk [a,b], Antoni C.G. van Ginneken [a,b], Géza Berecki [a,b], Hester M. den Ruijter [a], Cees A. Schumacher [a], Marieke W. Veldkamp [a], Antonius Baartscheer [a], Simona Casini [a], Tobias Opthof [a], Robert Hovenier [c], Jan W.T. Fiolet [a], Peter L. Zock [d], Ruben Coronel [a,*]

[a] *Experimental and Molecular Cardiology Group, Academic Medical Center, University of Amsterdam, Amsterdam, The Netherlands*
[b] *Department of Physiology, Academic Medical Center, University of Amsterdam, Amsterdam, The Netherlands*
[c] *Department of Nutrition, Faculty of Veterinary Medicine, Utrecht University, Utrecht, The Netherlands*
[d] *Department of Human Nutrition, the Wageningen Centre for Food Sciences, Wageningen University, Wageningen, The Netherlands*

Received 13 September 2005; received in revised form 10 February 2006; accepted 21 February 2006
Available online 28 February 2006
Time for primary review 27 days

Abstract

Background: Omega-3 polyunsaturated fatty acids (ω3-PUFAs) from fish oil reduce the risk of sudden death presumably by preventing life-threatening arrhythmias. Acutely administered ω3-PUFAs modulate the activity of several cardiac ion channels, but the chronic effects of a diet enriched with fish oil leading to ω3-PUFA-incorporation into the sarcolemma on membrane currents are unknown.
Methods: Pigs received a diet either rich in ω3-PUFAs or in ω9-fatty acids for 8 weeks. Ventricular myocytes (VMs) were isolated and used for patch-clamp studies.
Results: ω3-VMs contained higher amounts of ω3-PUFAs and had a shorter action potential (AP) with a more negative plateau than control VM. In ω3 VMs, L-type Ca^{2+} current ($I_{Ca,L}$) and Na^+–Ca^{2+} exchange current (I_{NCX}) were reduced by approximately 20% and 60%, respectively, and inward rectifier K^+ current (I_{K1}) and slow delayed rectifier K^+ current (I_{Ks}) were increased by approximately 50% and 70%, respectively, compared to control. Densities of rapid delayed rectifier K^+ current, Ca^{2+}-activated Cl^- current, and Na^+ current (I_{Na}) were unchanged, although voltage-dependence of I_{Na} inactivation was more negative in ω3 VMs.
Conclusions: A fish oil diet increases ω3-PUFA content in the ventricular sarcolemma, decreases $I_{Ca,L}$ and I_{NCX}, and increases I_{K1} and I_{Ks}, resulting in AP shortening. Incorporation of ω3-PUFAs in the sarcolemma may have consequences for arrhythmias independent of circulating ω3-PUFAs.

Keywords: Ion channels; Ion exchangers; Membrane potential; Repolarization; Ca^{2+} transients; Nutrition; Fatty acids

1. Introduction

Increased consumption of fish oil, rich in omega-3 (ω3) polyunsaturated fatty acids (PUFAs), reduces cardiovascular mortality, especially sudden cardiac death, in patients with healed myocardial infarction [1,2]. In rats fed a fish oil-rich diet the number of ischemia/reperfusion related arrhythmias is reduced [3]. The mechanisms underlying the anti-arrhythmic effect of a diet rich in ω3-PUFAs are unknown. Acutely administered ω3-PUFAs reversibly modulate a variety of cardiac ion channels and exchangers [4]. Long term electrophysiological effects of ω3-PUFA intake leading to incorporation of ω3-PUFAs into the sarcolemma have not been studied. Incorporation of ω3-PUFAs into the phospholipid bilayer affects sarcolemmal biophysical properties [5].

* Corresponding author. Academic Medical Center, Rm M0-108, Department of Experimental Cardiology, Meibergdreef 9, 1105 AZ Amsterdam, The Netherlands. Tel.: +31 20 5663267; fax: +31 20 6975458.
E-mail address: R.Coronel@amc.uva.nl (Ruben Coronel).

0008-6363/$ - see front matter © 2006 European Society of Cardiology. Published by Elsevier B.V. All rights reserved.
doi:10.1016/j.cardiores.2006.02.022

We hypothesize that incorporation of ω3-PUFAs in the absence of circulating fatty acids has electrophysiological effects on various cardiac ion channels and transporters. Therefore, we studied ion channel characteristics of cardiac ventricular myocytes (VMs) isolated from pigs fed for 8 weeks with a diet rich in either fish oil (ω3-PUFA) or in ω9 fatty acids (high oleic sunflower oil, HOSF) as a control. We show that incorporated sarcolemmal ω3-PUFAs alone result in action potential (AP) shortening, caused by combined effects on various Ca^{2+} and K^+ ion channels and the Na^+–Ca^{2+} exchanger. Therefore, incorporation of ω3-PUFAs into the sarcolemma may affect reentrant and triggered arrhythmias.

2. Methods

2.1. Cell preparation

The investigation conforms to the *Guide for the Care and Use of Laboratory Animals* (NIH Publication 85-23, 1996). Male pigs (7 weeks old) received a diet rich in ω3-PUFA or HOSF for 8 weeks. Table 1 summarizes the composition of these diets. Average body weight after 8 weeks of diet was similar in ω3-PUFA and HOSF fed animals (55.4 ± 1.8 vs. 52.3 ± 1.4 kg, mean ± S.E.M., $n = 8$).

After the feeding period, pigs were sedated with ketamine (500 mg, i.m. Nimatek; Animal Health), azaperon (160 mg, i.m. Stresnil; Janssen-Cilag) and atropine (0.5 mg, i.m.; Centrafarm) and anaesthetized with pentobarbital (20 mg/kg, i.v. Nembutal; Ceva Sante Animale). A side-branch of the circumflex artery was cannulated and the perfused myocardium was moved to a perfusion setup. Left midmyocardial VMs were enzymatically isolated as described previously [6]. Small aliquots of cell suspension were put in a recording chamber on the stage of an inverted microscope. Cells were allowed to adhere for 5 min before superfusion was initiated. The temperature was 35–36 °C, except for Na^+ current recordings (22–23 °C). Quiescent, rod-shaped cross-striated cells and smooth surface were selected for measurements.

Table 1
Composition of HOSF and ω3 diet (g/100 g feed (*% total dietary energy*))

	HOSF	ω3
Total fat	6.22 *(14.58)*	6.26 *(14.77)*
Saturated fatty acids		
Total	0.72 *(1.69)*	1.09 *(2.57)*
Monounsaturated fatty acids		
Total	3.82 *(9.02)*	1.08 *(2.54)*
C18:1ω9 (oleic acid)	3.73 *(8.80)*	0.73 *(1.73)*
Polyunsaturated fatty acids		
Total	1.40 *(3.31)*	3.02 *(7.12)*
C18:2ω6 (LA)	1.39 *(3.28)*	1.08 *(2.54)*
C18:3ω3 (ALA)	0.01 *(0.03)*	0.02 *(0.06)*
C20:4ω6 (AA)	0.00 *(0.00)*	0.06 *(0.13)*
C20:5ω3 (EPA)	0.00 *(0.00)*	0.81 *(1.92)*
C22:6ω3 (DHA)	0.00 *(0.00)*	0.71 *(1.67)*
Other, unidentified fatty acids	0.03 *(0.07)*	0.64 *(1.51)*
Total carbohydrate	64.80 *(67.5)*	64.80 *(67.5)*
Corn Starch	32.40 *(33.8)*	32.40 *(33.8)*
Glucose	32.40 *(33.8)*	32.40 *(33.8)*
Total proteins		
Casein	18.0 *(18.8)*	18.0 *(18.8)*
Total energy content (kJ)	16065	16065

HOSF = high oleic sunflower oil, ω3 = fish oil, LA = linoleic acid, ALA = α-linolenic acid; AA = arachidonic acid, EPA = eicosapentaenoic acid, DHA = docosahexaenoic acid. The sum of listed components is less than the totals indicated here, since not all components were analyzed.

2.2. Electrophysiology

2.2.1. Data acquisition and analysis

Membrane potentials and currents were recorded in the whole-cell configuration of the patch-clamp technique (Axopatch 200B Clamp amplifier, Axon Instruments Inc.) using patch pipettes (1–3 MΩ, borosilicate glass). Voltage control, data acquisition, and analysis were accomplished using custom software. Potentials were corrected for liquid junction potential, except for I_{Na} measurements where it was 0.2 mV. Membrane currents and potentials were low-pass filtered (1 kHz) and digitized (2 kHz), except for AP and I_{Na} measurements, 5 and 20 kHz, respectively. Cell membrane capacitance (C_m) was estimated as described previously [7]. Series resistance was compensated for by at least 80%.

2.2.2. Current clamp experiments

APs were elicited at 0.2 to 6 Hz by 3 ms, 1.5× threshold current pulses through the patch pipette. We analyzed resting membrane potential (RMP), maximal upstroke velocity, stimulation threshold, maximal AP amplitude, plateau amplitude (defined as the potential difference between RMP and potential 50 ms after the upstroke), and AP duration at 20%, 50%, and 90% repolarization. Parameters from 10 consecutive APs were averaged.

2.2.3. Voltage-clamp experiments

Na^+ current (I_{Na}), L-type Ca^{2+} current ($I_{Ca,L}$), T-type Ca^{2+} current ($I_{Ca,T}$), Ca^{2+}-activated Cl^- current ($I_{Cl(Ca)}$), inward rectifier K^+ current (I_{K1}), slow delayed rectifier K^+ current (I_{Ks}), rapid delayed rectifier K^+ current (I_{Kr}), and Na^+–Ca^{2+} exchange current (I_{NCX}) were measured with the solutions indicated below and by voltage-clamp protocols shown in the appropriate figures. Voltage-dependence of (in)activation was determined by fitting a Boltzmann function ($y = A/[1 + \exp\{(V - V_{1/2})/k\}]$) to the individual curves, yielding half-maximal voltage ($V_{1/2}$) and slope factor k. The time constants of recovery from inactivation were determined using a double-exponential function ($I_{Na} = [A_f \times \exp(-t/\tau_f)] + [A_s \times \exp(-t/\tau_s)]$), where t is the recovery time interval, τ_f and τ_s are the time constants of fast and slow components, and A_f and A_s are the fractions of the fast and slow components. Current densities were calculated by dividing current amplitudes by C_m.

2.2.4. Solutions

Standard pipette solution contained (mmol/L): K-gluconate 125, KCl 20, K_2-ATP 5, HEPES 10; pH 7.2 (KOH). EGTA (10 mmol/L) was added to the pipette solution for I_{Na}, $I_{Ca,T}$, $I_{Ca,L}$, I_{Kr} and I_{Ks} measurements. For I_{Na}, $I_{Ca,T}$ and $I_{Ca,L}$ measurements, CsCl replaced all K-gluconate and KCl in the pipette solution. Furthermore, for I_{Na} measurements K_2-ATP was replaced by Na_2-ATP (2 mmol/L) and NaCl (3 mmol/L). Standard Tyrode's solution contained (mmol/L): NaCl 140, KCl 5.4, $CaCl_2$ 1.8, $MgCl_2$ 1.0, glucose 5.5, HEPES 5.0; pH 7.4 (NaOH). $I_{Cl(Ca)}$was measured as the transient outward current sensitive to 0.2 mmol/L 4,4′diisothiocyanatostilbene-2,2′-disulfonic acid (DIDS). For $I_{Ca,T}$ and $I_{Ca,L}$ measurements, TEA-Cl and CsCl replaced NaCl and KCl of the bath solution, respectively. For I_{Na} measurements, NaCl was reduced to 7 mmol/L and KCl was replaced by CsCl (133 mmol/L). For I_{Na}, I_{Kr}, and I_{Ks} measurement, the bath solution included 5 μmol/L nifedipine. I_{Kr} was measured as 5 μmol/L E-4031-sensitive current while I_{Ks} was measured as 90 μmol/L chromanol 293B-sensitive current in the presence of 5 μmol/L E-4031. pH of both extracellular and pipette solution was adjusted with CsOH and NMDG-OH for I_{Na} and I_{Ca} measurements, respectively. For I_{NCX} recording, the pipette solution contained (mmol/L): CsCl 145, NaCl 5, Mg-ATP 10, TEA 10, HEPES 10, EGTA 20, $CaCl_2$ 10; pH 7.2 (NMDG-OH). To suppress membrane currents other than I_{NCX}, the following blockers were added to a K^+-free Tyrode's solution (mmol/L): $BaCl_2$ 1, CsCl 2, nifedipine 0.005, ouabain 0.1, DIDS 0.2. I_{NCX} was measured as 10 mmol/L Ni^{2+}-sensitive current during a descending voltage ramp protocol [8].

2.2.5. Drugs

All drugs used for cellular measurements were obtained from Sigma-Aldrich (MO, USA), except for E-4031 (Eisai Inc., NJ, USA) and chromanol 293B (Tocris Cookson Inc. MO, USA). DIDS was freshly prepared as 0.5 mol/L stock solution in DMSO. Nifedipine and chromanol 293B, respectively, were prepared as 5 mmol/L and 0.1 mol/L stock solutions in ethanol. E-4031 was prepared as 5 mmol/L stock solution in distilled water. All stock solutions were diluted appropriately before use. DIDS and nifedipine were stored in the dark.

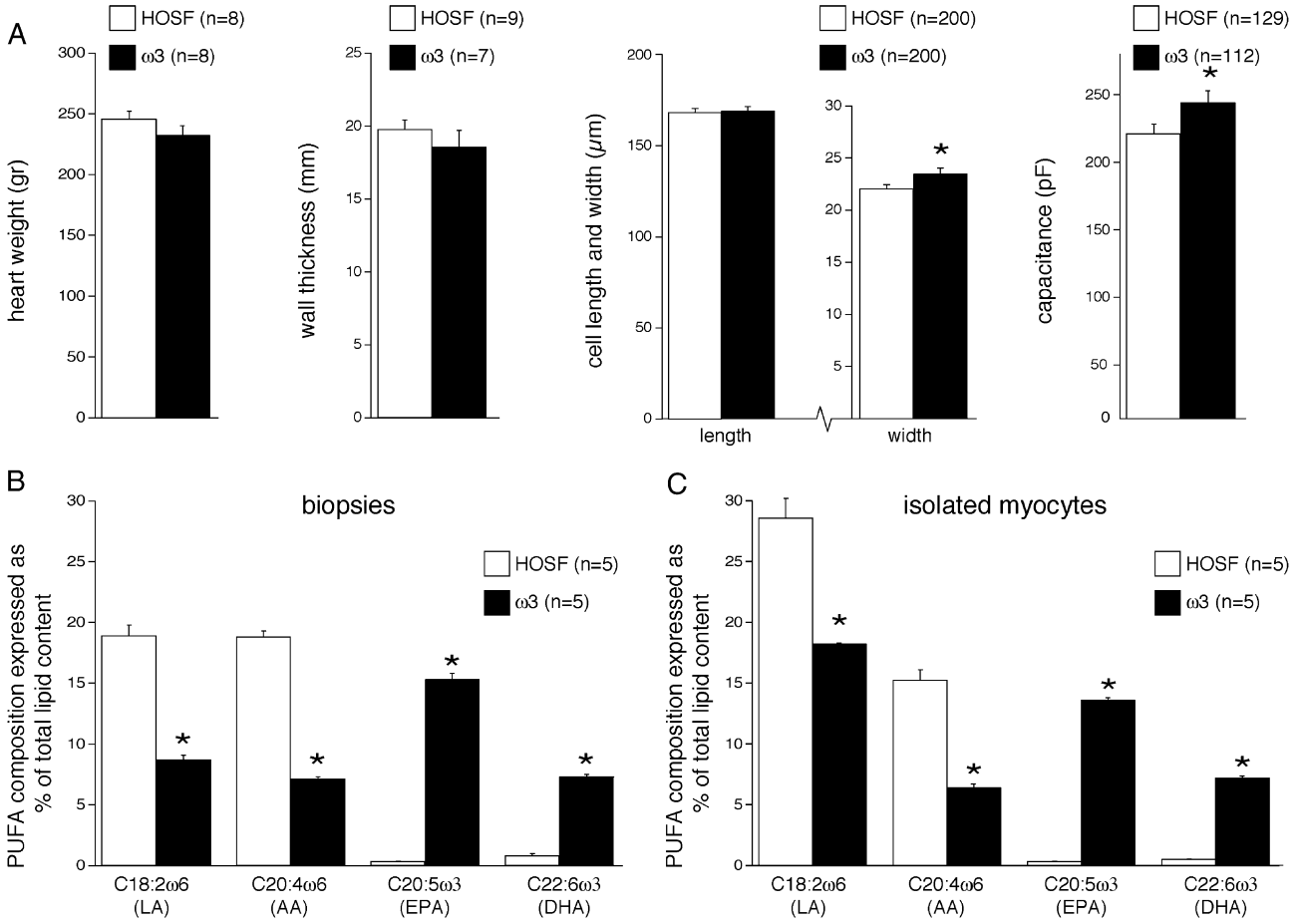

Fig. 1. Heart, cell, and membrane properties. (A) Morphological characteristics of heart and isolated VMs. *n*, number of hearts/myocytes (*$P<0.05$ unpaired *t*-test). (B and C) PUFA composition of VM membranes measured in biopsies (B) and isolated myocytes (C). *n*, number of hearts (*$P<0.05$ unpaired *t*-test).

2.3. Cytosolic Ca^{2+} measurements

Intracellular Ca^{2+}($[Ca^{2+}]_i$) was measured in indo-1 loaded VMs as described previously [9]. VMs were stimulated at 2 Hz with field stimulation. Dual wavelength emission of indo-1 was recorded ((405–440)/(505–540) nm, excitation at 340 nm) and free $[Ca^{2+}]_i$ was calculated [9].

2.4. Lipid analyses

Lipids from food, heart samples and myocytes were extracted with the method of Folch et al. [10]. Phospholipids from plasma and heart were isolated with aminopropyl bonded phase columns (Bond Elut; Varian BV). Saponification and methylation of the phospholipids with boron trifluoride (Pierce, IL, USA) was performed and the formed fatty acid methyl esters were subjected to capillary gas chromatography using a Chrompack column (Fused Silica, Chrompack), a flame ionization detector and H_2 as carrier gas. Fatty acid methyl esters were expressed as fraction of the total amount.

2.5. Statistics

Data are mean ± S.E.M. A *t*-test or in two-way Repeated Measures ANOVA followed by pairwise comparison using the Student–Newman–Keuls test was used. $P < 0.05$ defined statistical significance.

3. Results

3.1. Heart, cell, and membrane properties

3.1.1. Morphology

Fig. 1A summarizes basic heart and isolated VMs morphology characteristics of HOSF and ω3-PUFAs fed animals. Mean heart weight and left ventricular wall thickness were not different between the HOSF and ω3

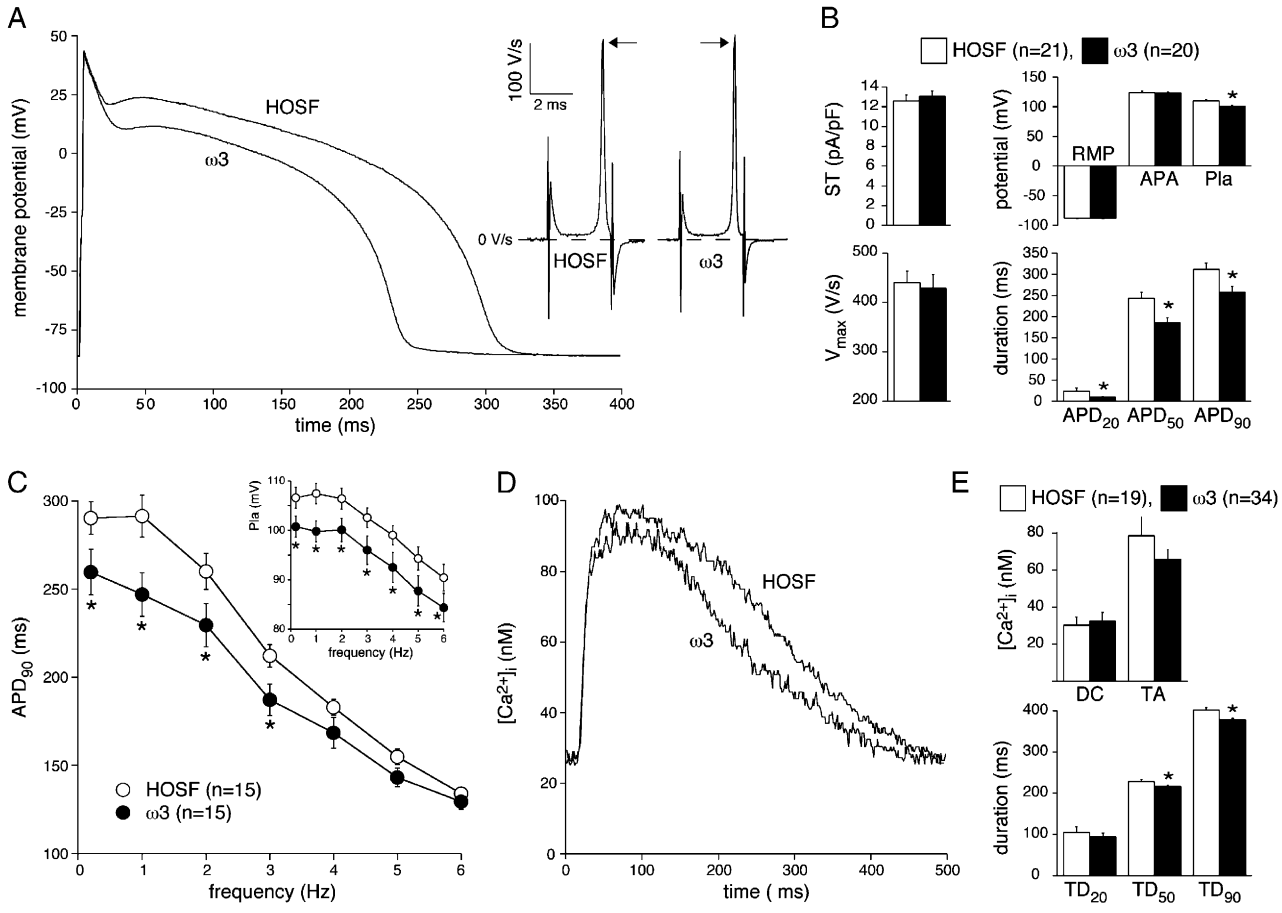

Fig. 2. Dietary ω3-PUFAs shorten action potentials (APs) and intracellular Ca^{2+}-transients. (A) Representative APs of a HOSF and an ω3 VM at 1 Hz. Inset shows maximal upstroke velocities (arrows). (B) Average AP parameters of HOSF and ω3 VMs. ST = stimulation threshold, V_{max} = maximal upstroke velocity, RMP = resting membrane potential, APA = maximal AP amplitude, Pla = AP plateau amplitude, APD_{20}, APD_{50}, and APD_{90} = AP duration at 20%, 50%, and 90% repolarization. *$P < 0.05$ in unpaired *t*-test. (C) Stimulus frequency-dependency of APD_{90} and Pla (inset) in HOSF and ω3 VMs. *$P < 0.05$ in ANOVA followed by Student–Newman–Keuls test. (D) Typical example $[Ca^{2+}]_i$-transients of a HOSF and an ω3 VM. (E) Average $[Ca^{2+}]_i$-transient parameters of HOSF- and ω3 VMs. DC = diastolic $[Ca^{2+}]_i$, TA = transient amplitude, TD_{20}, TD_{50}, and TD_{90} = transient duration at 20%, 50%, and 90% transient decrease. *$P < 0.05$ in unpaired *t*-test.

group. Cell length was similar, but cell width and C_m was significantly larger in ω3 VMs compared to HOSF.

3.1.2. PUFA composition

Fig. 1B summarizes the most prominent differences of cell phospholipid fraction in the two groups. In biopsies obtained from intact ω3 hearts as well as in isolated VMs, the proportion of ω3-PUFAs was increased at the expense of ω6-PUFAs. Thus, ω3-PUFAs from diet were incorporated in the cell membrane. Moreover, PUFA compositions in biopsies and isolated myocytes were similar (Fig. 1B), indicating that the cell isolation procedures did not affect the composition of the sarcolemma.

3.2. Action potentials and $[Ca^{2+}]_i$-transients

Fig. 2A shows representative APs at 1 Hz from a HOSF and ω3 VM. The ω3 AP has a more negative plateau potential and is considerably shorter than HOSF AP. Fig. 2B summarizes AP characteristics of HOSF and ω3 VMs. On average, ω3 VMs show a 10% more negative AP plateau potential and a 30% shorter AP at both 50% and 90%

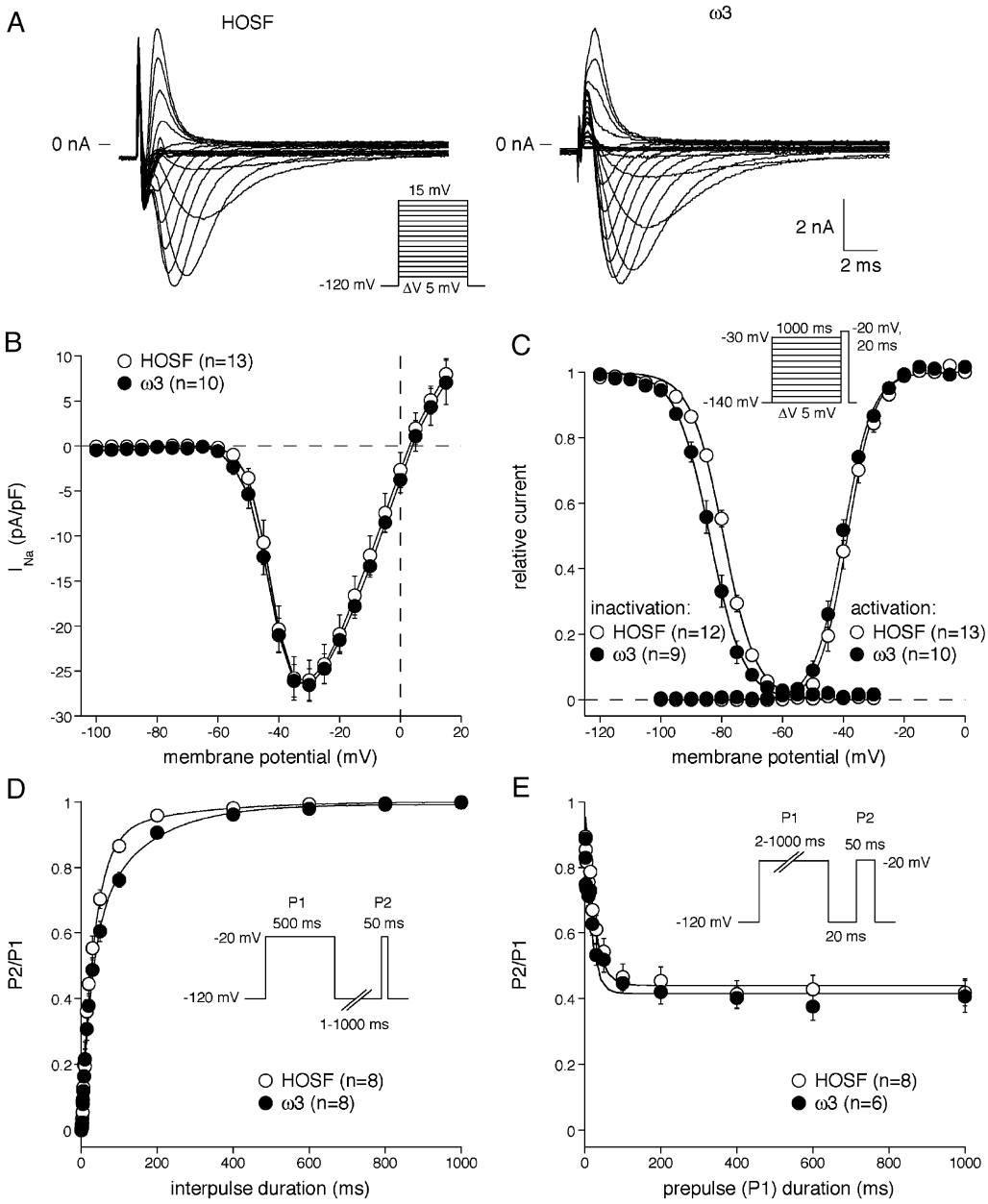

Fig. 3. Effect of dietary ω3-PUFAs on Na^+ current (I_{Na}). (A) Representative I_{Na} of a HOSF and ω3 VM. (B) Peak current–voltage ($I-V$) relationships of I_{Na}. (C) Voltage-dependence of (in)activation. Inactivation was approximately −4 mV shifted in ω3 VMs (*$P<0.05$). Solid lines: Boltzmann fits of the average data. (D) Recovery from inactivation. Solid lines: double-exponential functions of the average data (P=n.s. in ANOVA). (E) Development of slow inactivation of I_{Na}. Solid lines: mono-exponential functions of the average data. Insets: protocols used.

repolarization. No significant differences in RMP, excitability threshold, maximal upstroke velocity or maximal AP amplitude are observed. The AP shortening in ω3 VMs is particularly clear at physiological heart rates, i.e. at 3 Hz, and slower; the more negative AP plateau potential is present at all pacing frequencies (Fig. 2C). Fig. 2D shows typical $[Ca^{2+}]_i$-transients and Fig. 2E summarizes $[Ca^{2+}]_i$-transient characteristics of HOSF and ω3 VMs. No significant differences in diastolic $[Ca^{2+}]_i$ and $[Ca^{2+}]_i$-transient amplitudes are observed. The duration of $[Ca^{2+}]_i$-transient at both 50% and 90% of the transient decrease is significantly shorter in ω3 VMs.

3.3. Na^+ current

Fig. 3A shows representative I_{Na} recordings. Mean I_{Na} densities (Fig. 3B) are not different between HOSF and ω3 VMs. Peak I_{Na} averages -26.6 ± 1.8 and -26.1 ± 2.3 pA/pF in HOSF and ω3 VMs, respectively. Also voltage dependency of I_{Na} activation (Fig. 3C) does not differ significantly between HOSF and ω3 VMs. $V_{1/2}$ and k are -36.9 ± 0.6 mV and 4.8 ± 0.3 mV (HOSF) and -38.4 ± 0.5 mV and 4.9 ± 0.4 mV (ω3), respectively. Half-maximal inactivation voltages, based on current densities following a 1000-ms depolarizing prepulse, are -79.1 ± 0.8 mV (HOSF) and -83.5 ± 0.9 (ω3) ($P<0.05$). In HOSF and ω3 VMs, k's of inactivation are identical (-4.6 ± 0.1 mV (HOSF) vs. -4.9 ± 0.2 mV (ω3)). Recovery from inactivation (Fig. 3D) is not significantly different between HOSF and ω3 VMs. Double-exponential fits revealed that the time constants of fast and slow components of recovery (τ_{fast} and τ_{slow}, respectively) are 32.1 ± 4.1 and 1490 ± 205 ms in HOSF and 37.5 ± 3.6 and 1420 ± 372 ms in ω3 (both n.s.). Slow inactivation of I_{Na} (Fig. 3E) also is not significantly different between HOSF and ω3 VMs.

3.4. Ca^{2+} currents

3.4.1. T-type Ca^{2+} current

Fig. 4A shows representative I_{Ca} traces. The depolarizing steps from -90 and -50 mV to -20 mV elicit the time- and

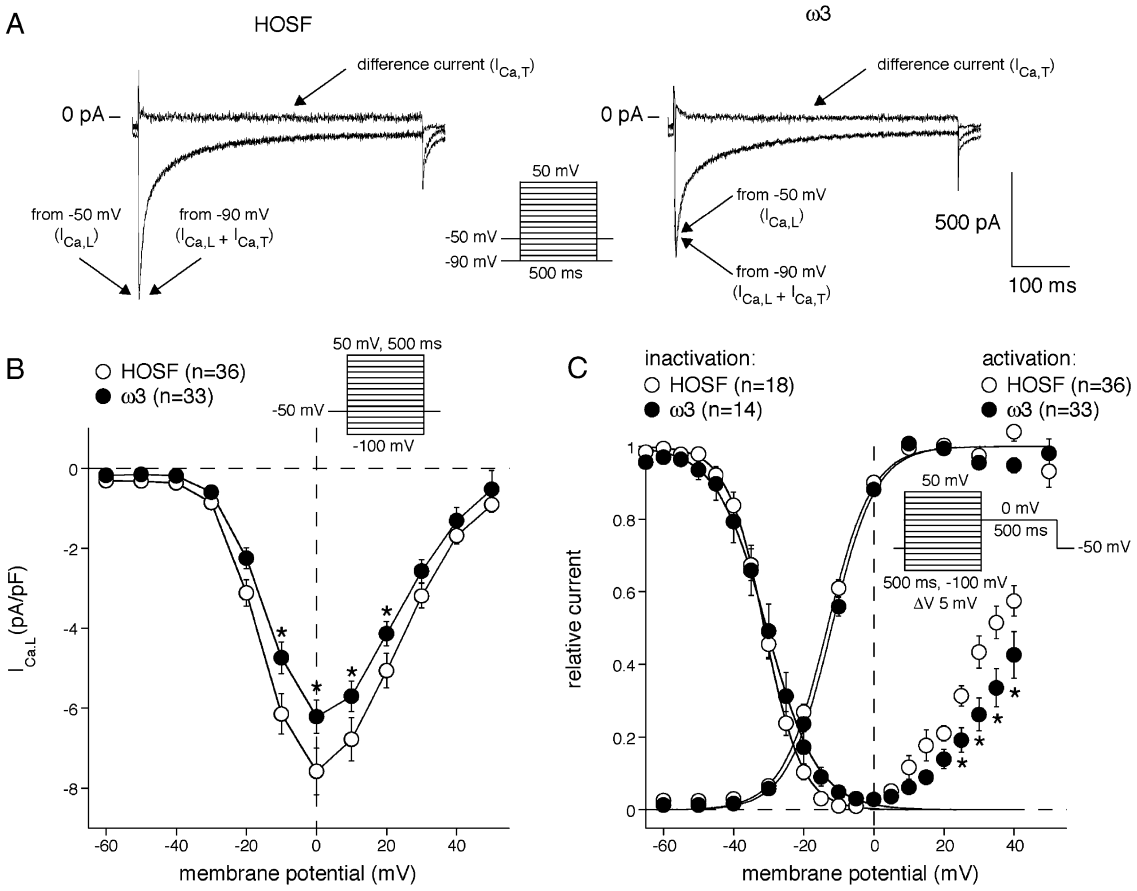

Fig. 4. Dietary ω3-PUFAs reduce L-type Ca^{2+} current ($I_{Ca,L}$) density. (A) Current traces elicited by depolarizing steps to -20 mV from -90 ($I_{Ca,L}$ and $I_{Ca,T}$) and -50 mV ($I_{Ca,L}$). $I_{Ca,T}$ was obtained by subtracting currents evoked from a HP of -50 mV from those with the same depolarization but evoked from a HP of -90 mV. Note that $I_{Ca,T}$ was absent. (B) Peak $I-V$ relationships of $I_{Ca,L}$. *$P<0.05$ in ANOVA followed by Student–Newman–Keuls test. (C) Voltage-dependence of $I_{Ca,L}$ (in)activation. Solid lines: Boltzmann fits of the average data. Activation and inactivation properties did not differ between HOSF and ω3 VMs, however, at ≥ 25 mV, where 'incomplete inactivation' occurs, $I_{Ca,L}$ was significantly smaller in ω3 VMs (*$P<0.05$ in ANOVA followed by Student–Newman–Keuls test).

voltage-dependent inward currents typical of I_{Ca}. $I_{Ca,T}$ is obtained by digital subtraction of I_{Ca} traces elicited by stepping from holding potentials of −90 and −50 mV. However, in both HOSF and ω3 VMs, the I_{Ca} traces from −90 and −50 mV are overlapping (Fig. 4A), indicating that $I_{Ca,T}$ was virtually absent in both cell types, in agreement with previous findings in adult VMs of other large mammals [11].

3.4.2. L-type Ca^{2+} current

$I_{Ca,L}$ is defined as I_{Ca} elicited from −50 mV and is significantly smaller in ω3 than HOSF VMs (Fig. 4A and B). For example, at 0 mV $I_{Ca,L}$ density averaged −7.6±0.6 (HOSF) and −6.2±0.4 pA/pF (ω3), indicating a 20% reduction of $I_{Ca,L}$ in ω3 VMs. The voltage-dependence of $I_{Ca,L}$ activation and inactivation are shown in Fig. 4C. Activation $V_{1/2}$ averaged −11.5±0.7 and −11.1±0.9 mV (P=n.s.). and slope factors are 6.2±0.2 and 6.2±0.1 mV (P=n.s., HOSF and ω3 VMs, respectively). Inactivation voltage-dependence was assessed with 500-ms prepulses followed by 500-ms test pulses to 0 mV (Fig. 4C, inset). Inactivation $V_{1/2}$ averages −28.3±1.1 (HOSF) vs. −28.4±1.6 mV (ω3, P=n.s.); slope factors are −4.8±0.2 and −4.6±0.1 mV (P=n.s.). Fig. 4C shows that the steady-state inactivation curve (or availability curve) rises positive to +10 mV, due to 'incomplete inactivation' [12]. Interestingly, in ω3 VMs, this 'incomplete inactivation' is significantly smaller than in HOSF VMs at potentials of +25 mV and more positive.

3.5. Cl^- currents

Fig. 5A shows superimposed current traces recorded in absence and presence of 0.2 mmol/L DIDS. By digitally subtracting the two traces (Fig. 5B), the DIDS-sensitive $I_{Cl(Ca)}$ is obtained [7]. $I_{Cl(Ca)}$ was found in all VMs, and exhibits similar current densities and I–V relationships in both groups (Fig. 5C). No DIDS-sensitive steady-state currents are observed, excluding the presence of persistently activated Cl^- currents [13].

3.6. K^+ currents

3.6.1. Inward rectifier K^+ current

I_{K1} is defined as steady-state current at the end of hyperpolarizing voltage-clamp steps from −40 mV [6]. The steady-state current is blocked by 2 mmol/L Ba^{2+}, and no time-dependent currents are observed in the presence of Ba^{2+} (Fig. 6A), excluding the contribution of the non-selective cation pacemaker current I_f to the steady-state current. Fig. 6B shows mean I–V relationships of I_{K1}. The I–V relationships have a reversal potential of −88 mV, which is close to E_K and the RMP, and demonstrates inward rectification, characteristic for I_{K1}. Both inward and outward I_{K1} components are significantly larger in ω3 VMs. Maximum outward I_{K1} density at −70 mV was increased by 54% in ω3 VMs (3.1±0.3 to 2.0±0.1 pA/pF).

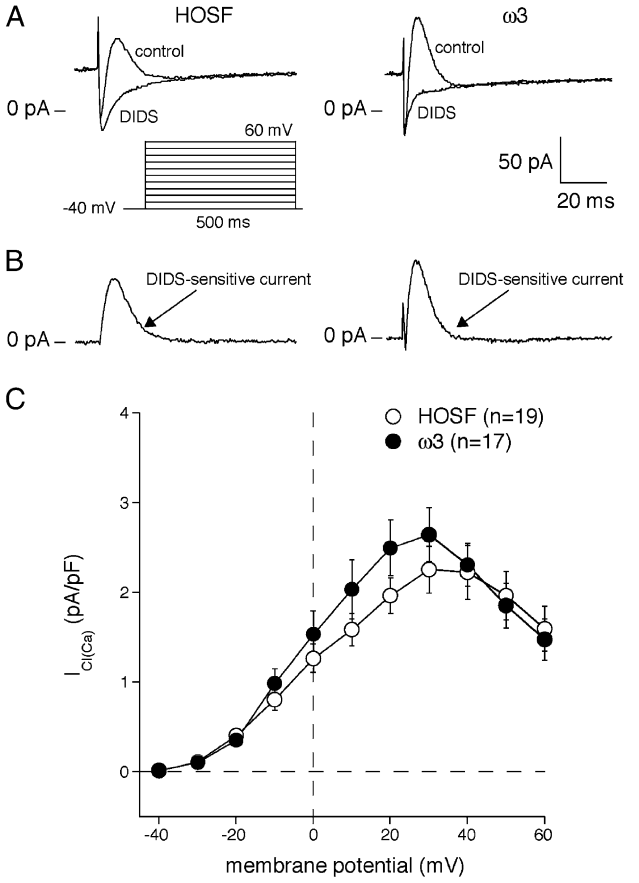

Fig. 5. Dietary ω3-PUFAs do not alter Ca^{2+}-activated Cl^- current ($I_{Cl(Ca)}$). (A) Current traces elicited by depolarizing voltage steps from −40 to 40 mV in absence and presence of 0.2 mmol/L DIDS. Inset: protocol used. (B) DIDS-sensitive current ($I_{Cl(Ca)}$). (C) Average I–V relationships of $I_{Cl(Ca)}$.

3.6.2. Delayed rectifier K^+ currents

Fig. 6C and D shows superimposed current traces recorded upon depolarizing steps from −50 to 0 mV (Fig. 6C) and from −50 to 40 mV (Fig. 6D) under control conditions, in the presence of E-4031, and in the combined presence of E-4031 and chromanol 293B to discriminate between I_{Kr} and I_{Ks}, respectively. I_{Kr} is defined as E-4031-sensitive current, and I_{Ks} as chromanol 293B-sensitive current. No change in mean I_{Kr} amplitude (Fig. 6E) is observed. Voltage-dependence of activation of I_{Kr} assessed by normalizing tail current amplitudes to maximum current is similar in HOSF and ω3 ($V_{1/2}$ and k, respectively, −36.8±2.0 and 10.0±1.4 mV (HOSF) and −37.1±2.3 and 8.1±1.6 mV (ω3)). I_{Ks} density is significantly larger in ω3 VMs (Fig. 6F). I_{Ks} density at 40 mV is increased by 70% in ω3 VMs (1.16±0.2 in HOSF vs. 1.98±0.4 pA/pF in ω3 VMs). The increase in density is accompanied by a tendency to shift the activation voltage-dependence toward more negative potentials. $V_{1/2}$

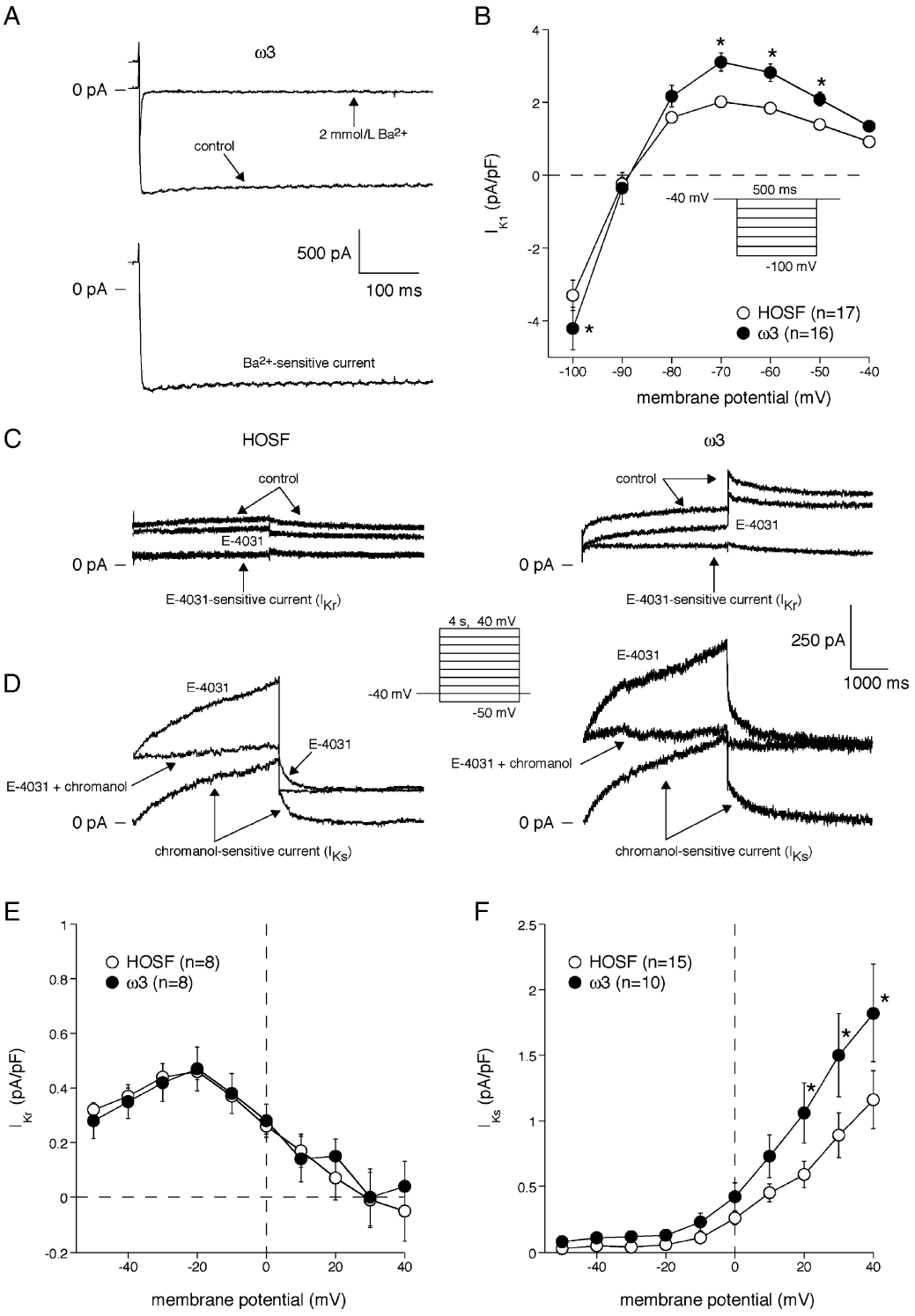

Fig. 6. Dietary ω3-PUFAs enhances slow delayed rectifier K^+ current (I_{Ks}) and inward rectifier K^+ current (I_{K1}) but not rapid delayed rectifier K^+ current (I_{Kr}). (A) Representative current traces elicited by a hyperpolarizing voltage step from −40 to −100 mV in control conditions and in presence of 2 mmol/L Ba^{2+}. (B) Average $I-V$ relationships of I_{K1}. (C) Representative current traces elicited by a voltage step from −50 to 0 mV in control conditions and in presence of 5 μmol/L E-4031. E-4031-sensitive current is defined as I_{Kr}. (D) Representative current traces elicited by a voltage step from −50 to 40 mV in presence of 5 μmol/L E-4031 and in the combined presence of 90 μmol/L chromanol-293B and E-4031. Chromanol 293B-sensitive current is defined as I_{Ks}. (E) Average $I-V$ relationships of I_{Kr}. (F) Average $I-V$ relationships of I_{Ks}. *$P<0.05$ in ANOVA followed by Student–Newman–Keuls test.

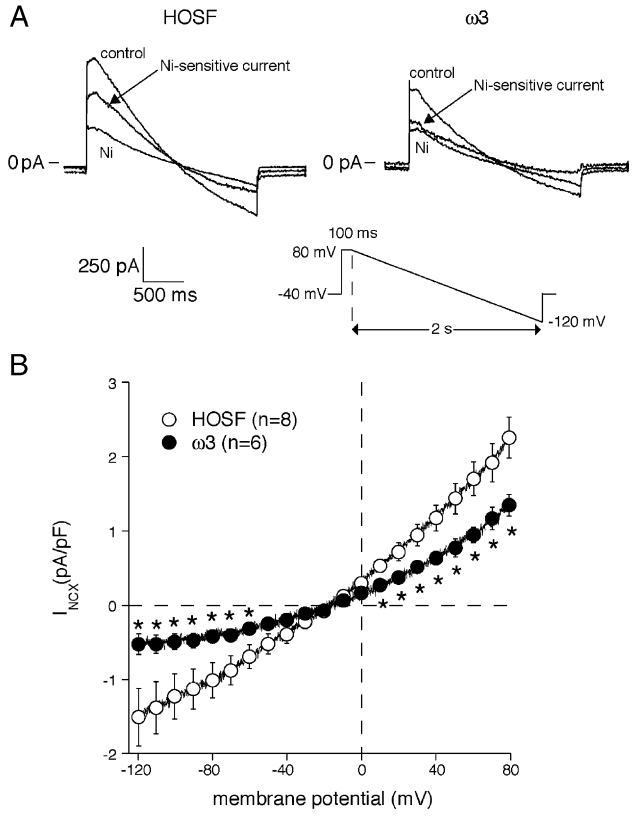

Fig. 7. Dietary ω3-PUFAs reduce Na^+–Ca^{2+} exchange current (I_{NCX}) density. (A) Typical current traces elicited by ramp protocol (inset) in absence and presence of 10 mmol/L $NiCl_2$, and the Ni^{2+}-sensitive current (I_{NCX}). (B) Average I–V relationships of I_{NCX}. *P<0.05 ANOVA followed by Student–Newman–Keuls test.

of I_{Ks} activation was 34.3±6.5 and 16.0±7.8 mV (P=0.07) in HOSF and ω3, respectively; k of I_{Ks} activation was identical (16.1±1.7 vs. 19.7±4.5 mV) in both groups.

3.7. Na^+–Ca^{2+} exchange current

Fig. 7A shows representative current traces in response to a descending voltage ramp protocol (Fig. 7A, inset) in the absence and presence of 10 mmol/L Ni^{2+}. I_{NCX} is measured as the Ni^{2+}-sensitive current [8]. In ω3 VMs (Fig. 7B), the current density of I_{NCX} is significantly reduced to 60% for the reverse (outward) mode (at +80 mV; 1.3±0.2 (ω3) vs. 2.3±0.3 (HOSF) pA/pF) and 31% for the forward (inward) mode (at −120 mV; −0.46±0.14 (ω3) vs. −1.5±0.4 (HOSF) pA/pF).

4. Discussion

Chronic feeding of a large mammal with fish oil leads to incorporation of ω3-PUFAs into the ventricular sarcolemma and at the same time induces various electrophysiological effects in the absence of circulating fatty acids. It decreases $I_{Ca,L}$ and I_{NCX}, increases I_{K1} and I_{Ks}, and causes AP shortening.

4.1. Comparison with previous studies of remodeling of membrane currents by ω3-PUFAs

We have studied the electrophysiological effects of incorporated sarcolemmal ω3-PUFAs, rather than the acute direct interaction between circulating ω3-PUFAs and the ion channels in the sarcolemma. We isolated the myocytes in the presence of lipid-free albumin, which removes loosely bound ω3-PUFAs from the cell surface [14]. Moreover, the experiments were performed with a PUFA-free superfusion solution. The cellular electrophysiological effects of ω3-PUFAs administered by diet are unknown.

A decrease in I_{Na} density after acute administration of ω3-PUFAs has been observed in isolated rat myocytes and HEK cells [15,16]. It was accompanied by a negative shift in voltage-dependence of inactivation. This increased the stimulation threshold and decreased V_{max} in cultures of neonatal myocytes [16]. In our study, no reduction I_{Na} density was found (Fig. 3B) and the shift in voltage-dependence of inactivation (Fig. 3C) was considerably smaller than that observed after acute administration of ω3-PUFAs [15]. As a consequence, we did not observe a significant change in stimulation threshold or upstroke velocity (Fig. 2B).

$I_{Ca,L}$ was smaller in ω3 than in HOSF VMs (Fig. 4B), in agreement with effects of acute administration of ω3-PUFAs [17]. Voltage-dependence of activation and inactivation of $I_{Ca,L}$ were not significantly different between the two groups (Fig. 4C). When the protocol used for determining inactivation was extended to more positive potentials, a ‘U-shaped curve’ was seen in both groups (Fig. 4C). The current increase at potentials positive to +10 mV is thought to be caused by reduced Ca^{2+} current-dependent inactivation [12], and was significantly smaller than in ω3 VMs. It suggests that the inward current caused by reopening of $I_{Ca,L}$ channels during the late plateau phase, is smaller. This might subsequently shorten AP (Fig. 2), and, more importantly, reduce the propensity to early afterdepolarizations (EADs) in ω3 VMs.

I_{K1} density was larger in ω3 VMs (Fig. 6B). The increased I_{K1} may result in earlier repolarization and a more stable resting membrane potential [18], the latter potentially protects against delayed afterdepolarizations (DADs).

The delayed rectifier K^+ currents, I_{Kr} and I_{Ks}, underlie repolarization of cardiac APs [18]. In our study, I_{Ks}, showed relatively the largest increase (70%) by ω3-PUFAs (Fig. 6F). The effects on I_{Ks} are similar to those after acute administration of docosahexanoic acid [19]. The increase in repolarizing current I_{Ks} contributes importantly to AP shortening (Fig. 2).

I_{NCX} was reduced both in the reversed and forward mode by the dietary ω3-PUFAs (Fig. 7), in line with the acute administration of ω3-PUFAs on I_{NCX} expressed in HEK cells [20]. The NCX maintains the Ca^{2+} balance of the VM by transport of Ca^{2+} across the membrane in exchange for

Na^+ [21]. Its activity is called "forward" when Ca^{2+} is transported outward. During the early phase of a cardiac AP, the NCX is briefly in reversed mode resulting in an outward current. During the plateau and final repolarizing phases of the AP, however, the NCX is in forward mode, resulting in depolarizing current [21]. The decreased I_{NCX} thus results in less depolarizing current during the final repolarizing phase of the AP, causing AP shortening. Moreover, I_{NCX} carries the transient inward current responsible for the DADs [21]. Decreased I_{NCX} may therefore result in decreased propensity to develop DADs.

The mechanism by which dietary ω3-PUFAs decrease I_{NCX} and $I_{Ca,L}$, increase I_{Ks} and I_{K1}, and leave other ionic currents unaltered remains to be elucidated. Evidence is accumulating that ω3-PUFAs alter different microdomains of the plasma membrane, such as lipid rafts and caveolae, thereby directly influencing protein function [4,5], but changes in PKC activation may also play a role [22]. The present study indicates that the role of changes in channel gating is limited, since activation and inactivation properties were hardly affected by dietary ω3-PUFAs. Further experiments are required to study the mechanism by which PUFAs alter ionic current densities.

4.2. Comparison with previous studies of action potential duration remodeling by ω3-PUFAs

Dietary ω3-PUFAs shortens ventricular APs of pigs (Fig. 2). To our knowledge, no other experimental findings on effects of ω3-PUFAs administered by diet on APs are available. Our findings are in line with the observation that rabbits on a diet enriched with α-linolenic acid (an ω3-PUFA) have shorter QTc intervals [23], but disagree with observations in healthy humans where dietary supplementation of ω3-PUFAs did not alter QTc intervals [24]. Acutely administered ω3-PUFAs also reduce AP duration in rabbit [23] and guinea pig [25] VMs. Interestingly, acute administration of ω3-PUFAs (>10 μM) reduces [25], whereas lower concentrations prolong AP duration in rat VMs [17].

AP duration in rats and mice is determined by the transient outward K^+ current (I_{to1}), a current that is lacking in porcine ventricle [26]. It determines the plateau potential rather than AP duration in other (larger) mammalian species. The observed AP shortening in response to dietary ω3-PUFAs agrees with our findings of decreased inward currents, i.e. $I_{Ca,L}$ and I_{NCX} and increased repolarizing currents, i.e., I_{KS} and I_{K1} (see above).

4.3. Comparison with previous studies of altered $[Ca^{2+}]_i$ by ω3-PUFAs

The AP shortening induced by dietary ω3-PUFAs is likely due to changes in $I_{Ca,L}$, I_{NCX}, I_{KS}, and I_{K1} densities. However, these currents were measured with EGTA in the pipette solution, while the APs were recorded without EGTA. In addition to changes in current densities, changes in $[Ca^{2+}]_i$, might also contribute to the AP shortening by modulation of membrane currents [27]. Diastolic $[Ca^{2+}]_i$ and $[Ca^{2+}]_i$-transient amplitudes, however, were similar in HOSF and ω3 VMs (Fig. 2). This agrees with results in rats [28], but contrasts with data obtained following acute administration of ω3-FUFAs. There, a rapid decrease in diastolic $[Ca^{2+}]_i$ and negative inotropic effect ensued [25,29]. We observed a shorter $[Ca^{2+}]_i$-transient in ω3 VMs. Whether this occurred due to altered SR function [28] or to AP shortening by itself [24] is not known. The earlier occurrence of phase-3 repolarization by itself would reduce $[Ca^{2+}]_i$ via modulation of the NCX and cause a shorter $[Ca^{2+}]_i$-transient [25].

4.4. (Patho)physiological implications

Our results suggest that incorporated sarcolemmal ω3-PUFAs, as a result of a fish oil-rich diet, may have distinct consequences for arrhythmogenesis. The increase in K^+ current density and decrease of I_{NCX} and $I_{Ca,L}$ most likely contribute importantly to AP shortening and may *facilitate* rather than *prevent* reentrant arrhythmias [30]. On the other hand, AP shortening may also reduce the occurrence of triggered activity based on EADs [31]. EADs constitute an important cellular mechanism for triggered activity, which may trigger life-threatening ventricular arrhythmias in patients with heart failure and/or long QT-syndromes [32]. The occurrence of EADs is likely to be further prevented by the reduction of $I_{Ca,L}$ by dietary ω3-PUFAs [17,18]. The ω3-PUFAs-induced reduction of EADs is supported by preliminary results in rabbit hearts where the ω3-PUFA diet reduced the occurrence of Torsades de Pointes arrhythmias [33], which are importantly due to EADs [34]. AP shortening, increase of I_{K1}, and decrease of I_{NCX} potentially protects against DADs evoked by high heart rates in Ca^{2+}-overload conditions [18]. Finally, the negative shift of the I_{Na} inactivation curve indicates that at a certain degree of depolarization (that occurs in acute myocardial ischemia) fewer Na^+ channels are available, causing conduction slowing and block. This may be potentially proarrhythmic [35].

4.5. Limitations of the study

We studied porcine VMs. The configuration of the human AP is very much like that of pig, but this does not exclude differences in the underlying membrane currents and thereby of the overall effects ω3-PUFAs have [18]. Further studies are required to clarify the effects of dietary ω3-PUFAs on I_{to1} (because the latter is lacking in porcine ventricle [26]) and on human VM electrophysiology.

Although feeding pigs with fish oil leads to major electrophysiological alterations due to incorporation of ω3-PUFAs into the membrane alone, additional effects of circulating ω3-PUFAs may be important as well.

5. Conclusions

Incorporated ω3-PUFAs in the absence of circulating ω3-PUFAs causes AP shortening. Based on the underlying changes in the profile of ionic sarcolemmal currents, we speculate that a fish oil-rich diet may have pro-arrhythmic as well as anti-arrhythmic consequences. This may explain why ω3-PUFAs seem protective against arrhythmias in patients with healed infarction (and with heart failure), but inefficient in patients with acute ischemia (angina pectoris). Thus, the impact of a fish oil enriched diet may depend on the pathophysiological setting.

Acknowledgements

We thank J. Zegers for kindly providing the data-acquisition program and F.J. Wilms-Schopman, C.N. Belterman, D. Bakker, and W.L. ter Smitte for their valuable help. This study was funded by the Wageningen Centre for Food Sciences, an alliance of major Dutch food industries, Maastricht University, TNO Nutrition and Food Research, and Wageningen University and Research Centre, with financial support by the Dutch government, and by the Netherlands Heart Foundation (2003B079) and SEAFOOD-plus program of the European Union (506359).

References

[1] GISSI-Prevenzione Investigators. Dietary supplementation with $n-3$ polyunsaturated fatty acids and vitamin E after myocardial infarction: results of the GISSI-Prevenzione trial. Lancet 1999;354:447–55.
[2] Burr ML, Fehily AM, Gilbert JF, Rogers S, Holliday RM, Sweetnam PM, et al. Effects of changes in fat, fish, and fibre intakes on death and myocardial reinfarction: diet and reinfarction trial (DART). Lancet 1989;2(8666):757–61.
[3] McLennan PL. Relative effects of dietary saturated, monounsaturated, and polyunsaturated fatty acids on cardiac arrhythmias in rats. Am J Clin Nutr 1993;57:207–12.
[4] Leaf A, Xiao Y-F, Kang JX, Billman GE. Prevention of sudden cardiac death by $n-3$ polyunsaturated fatty acids. Pharmacol Ther 2003;98:355–77.
[5] Ma DWL, Seo J, Switzer KC, Fan Y-Y, McMurray DN, Lupton JR, et al. $n-3$ PUFA and membrane microdomains: a new frontier in bioactive lipid research. J Nutr Biochem 2004;15:700–6.
[6] Veldkamp MW, Verkerk AO, van Ginneken ACG, Baartscheer A, Schumacher C, de Jonge N, et al. Norepinephrine induces action potential prolongation and early afterdepolarizations in ventricular myocytes isolated from human end-stage failing hearts. Eur Heart J 2001;22:955–63.
[7] Verkerk AO, Tan HL, Ravesloot JH. Ca^{2+}-activated Cl^- current reduces transmural electrical heterogeneity within the rabbit left ventricle. Acta Physiol Scand 2004;180:239–47.
[8] Hinde AK, Perchenet L, Hobai IA, Levi AJ, Hancox JC. Inhibition of Na/Ca exchange by external Ni in guinea-pig ventricular myocytes at 37 °C, dialysed internally with cAMP-free and cAMP-containing solutions. Cell Calcium 1999;25:321–31.
[9] Baartscheer A, Schumacher CA, van Borren MMGJ, Belterman CNW, Coronel R, Fiolet JWT. Increased Na^{+}/H^{+}-exchange activity is the cause of increased $[Na^+]_i$ and underlies disturbed calcium handling in the rabbit pressure and volume overload heart failure model. Cardiovasc Res 2003;57:1015–24.
[10] Folch J, Lees M, Sloane Stanley GH. A simple method for the isolation and purification of total lipids from animal tissues. J Biol Chem 1957;226:497–509.
[11] Perez-Reyes E. Molecular physiology of low-voltage-activated T-type calcium channels. Physiol Rev 2003;83:117–61.
[12] Tillotson D. Inactivation of Ca conductance dependent on entry of Ca ions in molluscan neurons. Proc Natl Acad Sci 1979;76:1497–500.
[13] Clemo HF, Stambler BS, Baumgarten CM. Swelling-activated chloride current is persistently activated in ventricular myocytes from dogs with tachycardia-induced congestive heart failure. Circ Res 1999;84:157–65.
[14] Kang JX, Leaf A. Effects of long-chain polyunsaturated fatty acids on the contraction of neonatal rat cardiac myocytes. Proc Natl Acad Sci 1994;91:9886–90.
[15] Leifert WR, McMurchie EJ, Saint DA. Inhibition of cardiac sodium currents in adult rat myocytes by $n-3$ polyunsaturated fatty acids. J Physiol 1999;520:671–9.
[16] Xiao Y-F, Kang JX, Morgan JP, Leaf A. Blocking effects of polyunsaturated fatty acids on Na^+ channels of neonatal rat ventricular myocytes. Proc Natl Acad Sci 1995;92:11000–4.
[17] Xiao Y-F, Gomez AM, Morgan JP, Lederer WJ, Leaf A. Suppression of voltage-gated L-type Ca2+ currents by polyunsaturated fatty acids in adult and neonatal rat ventricular myocytes. Proc Natl Acad Sci 1997;94:4182–7.
[18] Roden DM, Balser JR, George AL Jr, Anderson ME. Cardiac ion channels. Annu Rev Physiol 2002;64:431–75.
[19] Doolan GK, Panchal RG, Fonnes EL, Clarke AL, Williams DA, Petrou S. Fatty acid augmentation of the cardiac slowly activating delayed rectifier current (I_{Ks}) is conferred by hminK. FASEB J 2002;16:1662–4.
[20] Xiao Y-F, Ke Q, Chen Y, Morgan JP, Leaf A. Inhibitory effect of $n-3$ fish oil fatty acids on cardiac Na^+/Ca^{2+} exchange currents in HEK293t cells. Biochem Biophys Res Commun 2004;321:116–23.
[21] Blaustein MP, Lederer WJ. Sodium/calcium exchange: its physiological implications. Physiol Rev 1999;79:763–854.
[22] Judé S, Roger S, Martel E, Besson P, Richard S, Bougnoux P, et al. Dietary long-chain omega-3 fatty acids of marine origin: a comparison of their protective effects on coronary heart disease and breast cancers. Prog Biophys Mol Biol 2006;90:299–325.
[23] Ander BP, Weber AR, Rampersad PP, Gilchrist JS, Pierce GN, Lukas A. Dietary flaxseed protects against ventricular fibrillation induced by ischemia–reperfusion in normal and hypercholesterolemic rabbits. J Nutr 2004;134:3250–6.
[24] Geelen A, Brouwer IA, Zock PL, Kors JA, Swenne CA, Katan MB, et al. ($n-3$) Fatty acids do not affect electrocardiographic characteristics of healthy men and women. J Nutr 2002;132:3051–4.
[25] Macleod JC, Macknight ADC, Rodrigo GC. The electrical and mechanical response of adult guinea pig and rat ventricular myocytes to ω3 polyunsaturated fatty acids. Eur J Pharmacol 1998;356:261–70.
[26] Li G-R, Du X-L, Siow YL, K O, Tse H-F, Lau CP. Calcium-activated transient outward chloride current and phase 1 repolarization of swine ventricular action potential. Cardiovasc Res 2003;58:89–98.
[27] Carmeliet E. Intracellular Ca^{2+} concentration and rate adaptation of the cardiac action potential. Cell Calcium 2004;35:557–73.
[28] Leifert WR, Dorian CL, Jahangiri A, McMurchie EJ. Dietary fish oil prevents asynchronous contractility and alters Ca^{2+} handling in adult rat cardiomyocytes. J Nutr Biochem 2001;12:365–76.
[29] Negretti N, Perez MR, Walker D, O'Neill SC. Inhibition of sarcoplasmic reticulum function by polyunsaturated fatty acids in intact, isolated myocytes from rat ventricular muscle. J Physiol 2000;523:367–75.
[30] Janse MJ, Wit AL. Electrophysiological mechanisms of ventricular arrhythmias resulting from myocardial ischemia and infarction. Physiol Rev 1989;69:1049–169.

[31] Ducceschi V, Di Micco G, Sarubbi B, Russo B, Santangelo L, Iacono A. Ionic mechanisms of ischemia-related ventricular arrhythmias. Clin Cardiol 1996;19:325–31.
[32] Janse MJ. Electrophysiological changes in heart failure and their relationship to arrhythmogenesis. Cardiovasc Res 2004;61:208–17.
[33] Dujardin K, Dumotier B, Hondeghem L. Dietary supplementation with n-3 polyunsaturated fatty acids: a far less toxic alternative and perhaps superior antiarrhythmic therapy to amiodarone? Circulation 2005;112(Suppl. S):U554–U554 2368 [abstract].
[34] Yan GX, Wu Y, Liu T, Wang J, Marinchak RA, Kowey PR. Phase 2 early afterdepolarization as a trigger of polymorphic ventricular tachycardia in acquired long-QT syndrome: direct evidence from intracellular recordings in the intact left ventricular wall. Circulation 2001;103:2851–6.
[35] Preliminary report: effect of encainide and flecainide on mortality in a randomized trial of arrhythmia suppression after myocardial infarction. The Cardiac Arrhythmia Suppression Trial (CAST) Investigators. N Engl J Med 1989;321:406–12.